Journal of Alloys and Compounds 506 (2010) 243–248

Contents lists available at ScienceDirect

Journal of Alloys and Compounds

journal homepage: www.elsevier.com/locate/jallcom

Synthesis, characterization and properties of $Ln(Ti_{0.8}Sn_{0.2})TaO_6$ (Ln = Nd, Sm) microwave ceramics

Sam Solomon*

Department of Physics, St. John's College, Anchal 691306, Kerala, India

ARTICLE INFO

Article history:
Received 30 March 2010
Received in revised form 22 June 2010
Accepted 29 June 2010
Available online 7 July 2010

Keywords:
Ceramics
Microwave
Spectroscopy
Photoluminescence

ABSTRACT

The $Ln(Ti_{0.8}Sn_{0.2})TaO_6$ (Ln = Nd, Sm) ceramics are prepared through the solid-state ceramic route. The structure of the materials is studied using X-ray diffraction and Raman spectral analysis. The microstructure is analyzed using scanning electron microscopy and the elemental composition by energy dispersive spectrometry. The dielectric properties in the radio as well as in the microwave frequencies are studied. The photoluminescence property of the samples is also analyzed. The materials have dielectric constants 32.3 and 31.1, temperature coefficient of resonant frequency +1.5 ppm/K and −6 ppm/K and high quality factor and hence suitable for the fabrication of devices in microwave communication. Moreover, the compounds are useful in the field of optoelectronics since they produce intense emission lines in the visible region.

1. Introduction

Polycrystalline ceramic materials have widespread applications in the field of microwave communication and optoelectronics. Materials with low loss, high permittivity (ε_r) and low temperature coefficient of resonant frequency (τ_f) are useful as dielectric resonators in microwave devices. These requirements can be achieved by suitable substitution and doping. The ceramics which can absorb energy and subsequently emit the absorbed energy as light can be made useful in the fabrication of ceramic lasers.

The $A^{3+}B^{4+}C^{5+}O_6$ combination constitutes a special group of ceramics, whose phase pure existence was first established by Kazantsev et al. [1]. The crystal structure [2,3] and the microwave dielectric properties [4,5] of $LnTiTaO_6$ (where Ln is a lanthanide) were reported earlier. Attempts were made to obtain desirable microwave dielectric properties by suitable substitution and doping in $LnTiTaO_6$ ceramics. Surendran et al. [6], Solomon et al. [7], Oishi et al. [8,9] and Padma Kumar et al. [10–12] have studied the substitutional effects of lanthanides in the A site. The τ_f was reduced to zero approximately without much compromise in the values of the ε_r and quality factor by these substitutions. As per the reports by Joseph et al. [13] and Oishi et al. [9], the ε_r and τ_f decrease with an increase in concentration of Ta in $LnTi(Nb/Ta)O_6$ ceramics. The partial substitutions of Sb for Ta and Zr for Ti were reported by Padma Kumar et al. [14] and Solomon et al. [15], respectively. Due to these substitutions, there was an increase in quality factor and a decrease in ε_r and τ_f. The doping effects of ZnO [16], WO_3 and MoO_3 [17] in $LnTiTaO_6$ ceramics were also reported. By the ZnO doping, the ε_r and quality factor were increased and the τ_f was decreased, with considerable reduction in the sintering temperature. The WO_3 and MoO_3 addition increased the quality factor and reduced the τ_f without much variation in ε_r. Since Ti and Sn are tetravalent elements with slightly different ionic radii, it is possible to replace Ti partially by Sn. The compound obtained by the substitution of 20% Sn in the Zr site of $ZrTiO_4$ [18] ceramic was reported as an excellent composition for microwave applications. The τ_f of $ZrTiO_4$ was reduced approximately to zero by this substitution. Hence it may be possible to reduce the positive τ_f of $LnTiTaO_6$ ceramics also by the partial substitution of Sn in the Ti site. Qi et al. [19] have reported the optical absorption and photoluminescence of $LnTiNbO_6$ crystals in 1997. Jacob et al. [20] have reported the photoluminescence and low frequency dielectric properties of $LnTiTaO_6$ (Ln = Ce, Pr, Sm) ceramics. Padma Kumar et al. [21] studied the effect of Bi substitution in the Ln site of these ceramics. A detailed structural analysis of $LnTiTaO_6$ ceramics has been carried out by Thorogood et al. [22], using synchrotron X-ray powder diffraction and neutron diffraction techniques. Recently, Solomon et al. [23] and Dhwajam et al. [24] have reported the microwave dielectric and optical properties, respectively, of $PrTiTaO_6$–$YTiNbO_6$ ceramic composites. This paper reports the synthesis, characterization, photoluminescence and microwave dielectric properties of Sn-substituted $LnTiTaO_6$ (Ln = Nd, Sm) ceramics for the first time.

2. Experimental

Conventional solid-state ceramic route was used to prepare polycrystalline samples. High purity Nd_2O_3, Sm_2O_3, TiO_2, SnO_2 (CDH, 99.9%) and Ta_2O_5 (NFC, 99.9%)

* Tel.: +91 09847314237; fax: +91 471 2532445.
E-mail address: samdmrl@yahoo.com.

0925-8388/$ – see front matter © 2010 Elsevier B.V. All rights reserved.
doi:10.1016/j.jallcom.2010.06.185

were weighed in stoichiometric ratios and mixed thoroughly in acetone medium in a ball mill for 2 h. The powder was dried and then calcined at 1200 °C for 4 h in electrically heated furnace. The calcined powder was again ground well for 2 h with acetone as the wetting medium. The specimen was again dried well and 5 wt% polyvinyl alcohol was added as a binder and again ground well and dried. The powder was then pressed at a pressure of 150 MPa using hydraulic press in the form of cylindrical pellets. The pellets were then sintered in a controlled heating schedule of 4 °C/min up to 600 °C and soaked for an hour to expel the binder. This was followed by heating the samples at a rate of 5 °C/min up to 1380 °C with a soaking time of 4 h. The samples were then furnace cooled to room temperature.

The sintered densities of the well-polished samples were measured using Archimedes method. The sintered pellets were powdered in an agate mortar and used for X-ray diffraction (Philips Expert Pro) studies using Cu K_α radiation. Polished samples, thermally etched at 1320 °C for 30 min, were used for Scanning Electron Microscopy (SEM) (JEOL JSM 5610 LV). The dielectric constant and the quality factor of the samples were measured in the microwave frequency range using cavity resonator method with the network analyzer (Agilent 8753 ET). For this the specimen was placed on a quartz cylinder placed at the center of a cylindrical brass cavity whose diameter is 3–4 times greater than that of the sample. The microwave signal was coupled to the specimen through loop probes and $TE_{01\delta}$ mode of resonance whose quality factor is intimately related to the dielectric loss was identified. The temperature coefficient of resonant frequency (τ_f) was also measured over 30–70 °C with the heating setup attached to the computer interfaced network analyzer.

For radio frequency dielectric studies, thin pellets were made in the form of a disc capacitor with the specimen as the dielectric medium. The capacitance and conductance of the samples were measured using an LCR meter (Hioki-3532-50) within the frequency range 1 kHz to 1 MHz. The absorption spectra of the samples were recorded using Double beam UV–vis spectrometer Jasco-D550. The photoluminescence spectra of the samples were recorded using Flurolog®-3 Spectroflurometer. Raman spectra of selected samples were recorded and analyzed with a Bruker RFS100/S spectrometer (resolution of 4 cm^{-1} from 50 to 1000 cm^{-1} using Nd:YAG laser source, lasing at 1064 nm and power 150 mW and by a germanium diode detector).

3. Results and discussion

The XRD patterns of $Nd(Ti_{0.8}Sn_{0.2})TaO_6$ (NTST) and $Sm(Ti_{0.8}Sn_{0.2})TaO_6$ (STST) ceramics are given in Fig. 1. As per earlier reports [1,5] the $LnTiTaO_6$ with Ln = Ce, Pr, Nd, Sm, Eu, Gd, Tb and Dy crystallize in the orthorhombic structure with aeschynite symmetry and with Ln = Ho, Er, Yb and Y crystallize in the orthorhombic with the euxenite symmetry. The XRD peaks are indexed on the basis of the ICDD file numbers 20-1361 and 32-1452. The euxenite reflections are marked as (*) in the pattern. Both the samples show reflections prominently of aeschynite symmetry. There are some reflections of orthorhombic euxenite symmetry also. The euxenite reflections are more in STST when compared to NTST compositions. This may be due to the lesser ionic radius of Sm than that of Nd. The tendency to become euxenite from aeschynite increases with the decrease in ionic radii of lanthanides [5]. The structure is further confirmed using Raman spectra given in Fig. 2. Paschoal et al. [25] have reported the Raman spectra of $RETiTaO_6$ (RE = Ce, Pr, Nd, Sm, Eu, Gd, Tb, Dy, Ho, Er, Yb and Y) and have clearly differentiated the features of the characteristic Raman bands of both the structures. Accordingly Nd and Sm compounds have aeschynite structure and positive τ_f values. The Raman spectra recorded in the present study, for NTST and STST show good resemblance to that reported for the corresponding compounds [25] except for some of the bands. The region of the stretching vibrations of the TaO_6 octahedron itself is highly characteristic in both the structures. The symmetric stretching A_{1g} mode, which is the highest wavenumber band, is weak in the aeschynite structure but is highly intense and has a component to the lower wavenumber side around 790 cm^{-1} in the euxenite structure. The asymmetric stretching E_g mode is intense in the aeschynite while it is less intense and somewhat broad in the euxenite structure. In the present study, the intensity pattern of these two modes is in good agreement with that of the aeschynite structure. Paschoal et al. [25] have reported that the A_{1g} mode of the $NdTiTaO_6$ is at 864 cm^{-1} and that of $SmTiTaO_6$ is at 866 cm^{-1}. In the present study the corresponding band is

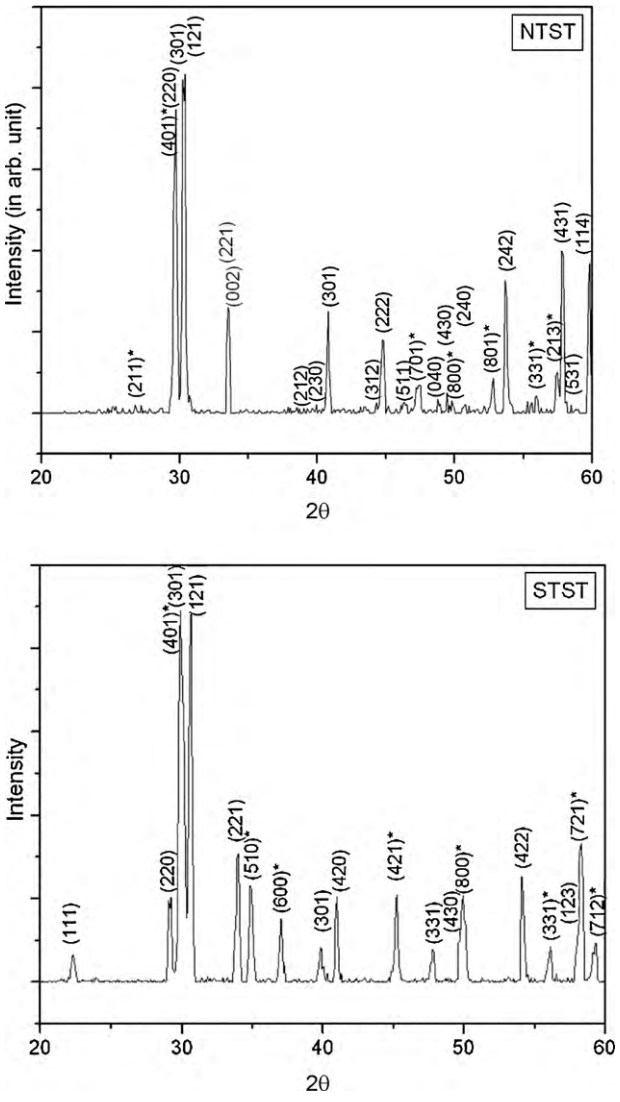

Fig. 1. The XRD patterns of NTST and STST ceramics.

observed at 863 cm^{-1} in NTST and at 851 cm^{-1} in STST. The shifting of the A_{1g} mode to the lower wavenumber side is a characteristic of euxenite structure. However, the E_g mode is observed at the same position as reported earlier—namely at 671 cm^{-1} in NTST and 675 cm^{-1} in STST. The band at 481 cm^{-1}, in the region of the bending vibrations of the octahedron, and the one at 118 cm^{-1} in STST are characteristics of euxenite structure. The medium intense band at 418 cm^{-1} in NTST indicates euxenite structure also in NTST.

The SEM images of NTST and STST ceramics are given in Fig. 3. From these images it is evident that the samples are sintered with minimum porosity. Most of the grains have the characteristic shape of aeschynite orthorhombic structured lanthanide titanium tantalates [8] with an average size of 1 μm. There are a few grains with different morphologies and it may be due to the co-existence of slight euxenite orthorhombic structure. Fig. 4 shows the EDS of NTST and STST ceramics. These spectra substantiate the presence of the stoichiometric concentrations of the constituents in the sample.

The microwave dielectric properties of the NTST and STST ceramics are given in Table 1. The $NdTiTaO_6$ has $\varepsilon_r = 43.1$ and $\tau_f = +30$ ppm/K and $SmTiTaO_6$ has $\varepsilon_r = 41.8$ and $\tau_f = +24$ ppm/K [5]. It can be observed that when 20% Sn is substituted for Ti the dielectric constant is decreased and thermal stability is achieved, still main-

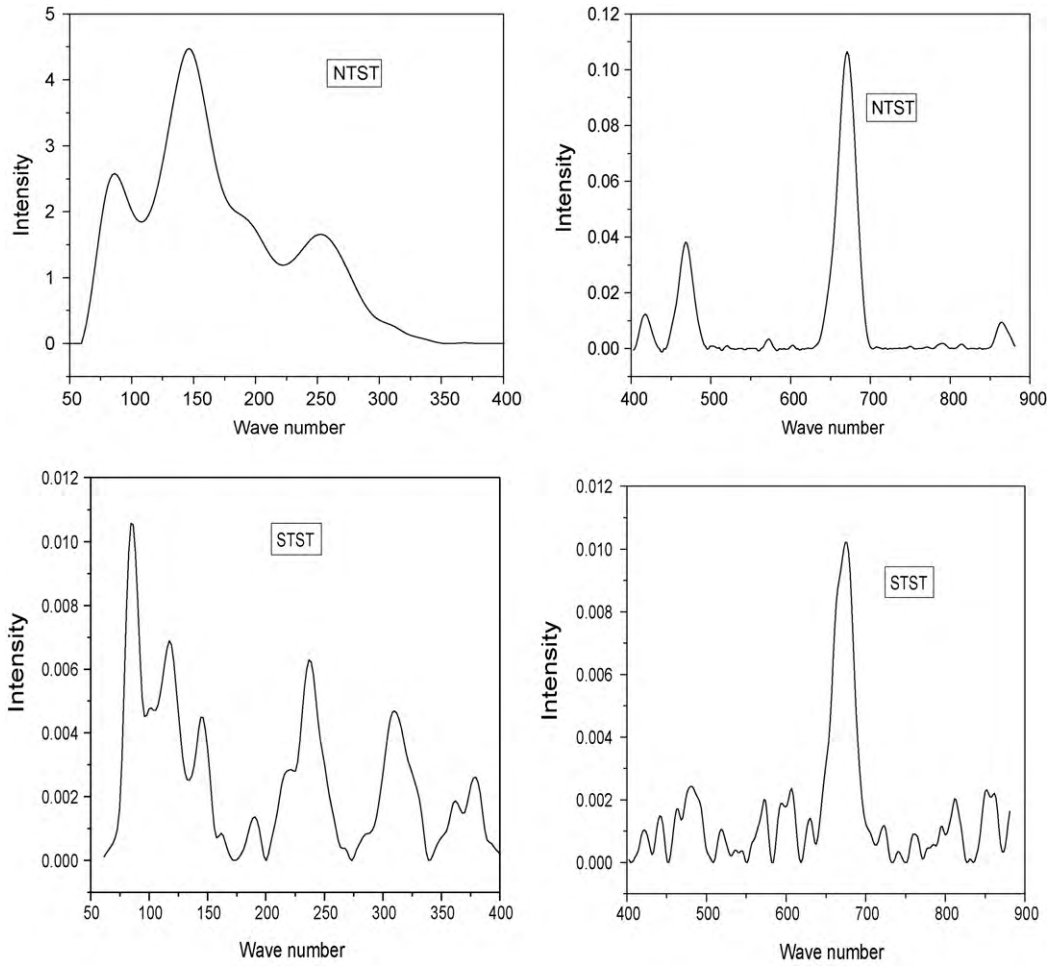

Fig. 2. Raman spectra of NTST and STST ceramics.

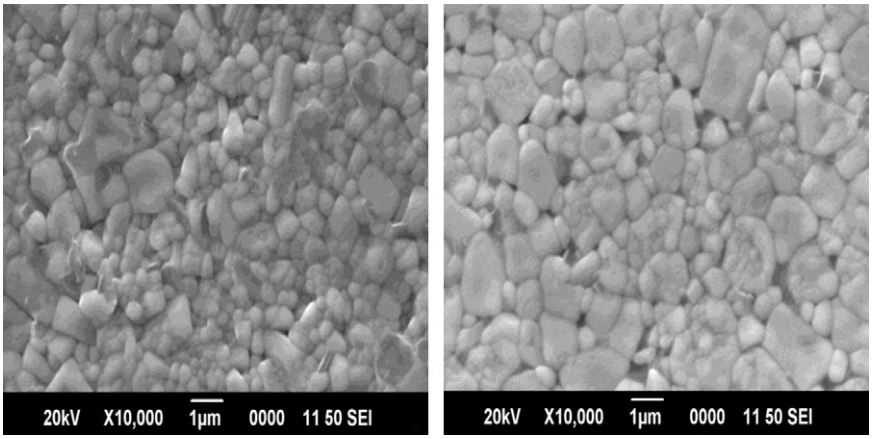

Fig. 3. SEM images of NTST and STST ceramics.

taining a high quality factor. In $LnTiTaO_6$ ceramics, the transition from aeschynite to euxenite structure occurs between Ln = Dy and Ln = Ho. For $DyTiTaO_6$ $\varepsilon_r = 34.6$ and $\tau_f = +7$ ppm/K and for $HoTiTaO_6$ $\varepsilon_r = 23.1$ and $\tau_f = -8$ ppm/K [5]. From Table 1 it is clear that the NTST and STST ceramics have ε_r and τ_f values between those of $DyTiTaO_6$ and $HoTiTaO_6$. Therefore we can expect a transition of symmetry from aeschynite to euxenite if the ε_r is between 34.6 and 23.1 and τ_f is between +7 and −8 ppm/K. Hence the microwave dielectric

Table 1
The microwave dielectric properties of the NTST and STST ceramics.

Compound	D (mm)	L (mm)	Density (g/cc)	Resonant frequency (GHz)	Dielectric constant	$Q \times f$ (GHz)	τ_f (ppm/K)
NTST	10.07	5.01	7.1	5.2981	32.3	24,160	+1.5
STST	10.18	4.72	7.35	5.4236	31.1	16,270	−6

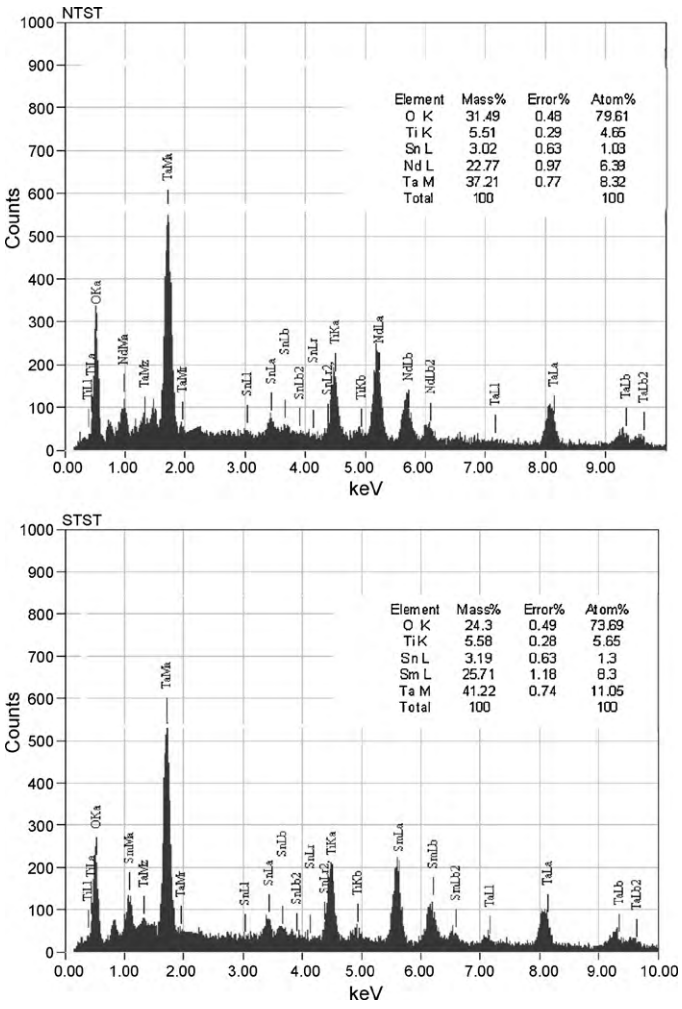

Fig. 4. EDS of NTST and STST ceramics.

properties of NTST and STST ceramics are in good agreement with the inference from X-ray diffraction analysis and Raman spectral analysis.

The variation in ε_r with respect to logarithm of frequency (log f), in the radio frequency region (1 KHz to 1 MHz) is given in Fig. 5. The ε_r decreases slightly with an increase in log f. This small variation

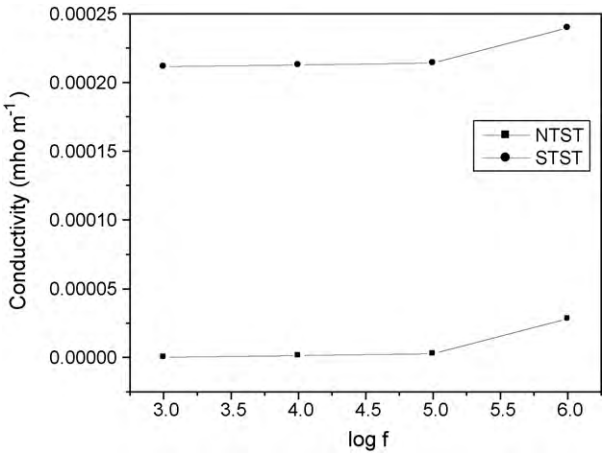

Fig. 6. Variation of conductance with log f in the radio frequency region.

confirms the highly sintered nature of the ceramic samples. The dielectric constant at 1 MHz and that at the microwave frequency are almost the same for NTST and some difference for STST. Fig. 6 shows the variation of conductivity with log f in the radio frequency region. This is complimentary to the variation in ε_r. Fig. 7 gives the variation in loss factor (tan δ) with respect to log f. The tan δ decreases with an increase in log f and minimum at 1 MHz.

The absorption spectra of the samples are given in Fig. 8. The bands are often broad and strongly influenced by chemical environmental factors. Both the samples have absorption bands in the visible region. As per the report by Jacob et al. [20] the $LnTiTaO_6$ ceramics have emission lines in the visible region. Fig. 9 gives the photoluminescence spectra of NTST and STST ceramics when excited by radiation of wavelength 400 nm. The samples have intense emission lines in the visible region. The transitions of the constituent elements of the compounds causing emission are identified on the basis of the data book by Payling and Larkins [26]. For NTST, the strong emission line at 454.9 nm can assign $^5I_6$–$^0A_5^0$ and/or $^5F_3$–$^5F_2^0$ and/or $^3P_0^0$–$^3D_1$ transitions. The weak emission line at 491.7 nm can assign $^4F_{1.5}$–$^2D_{2.5}^0$ transition. The strong emission line at 569 nm can assign $^2F_{2.5}$–$^0A_{2.5}^0$ transition. The emission line at 682 nm can assign $^4P_{2.5}$–$^4D_{3.5}^0$ transition. For STST the emission line at 478.5 nm and 529 nm can assign $^7F_2$–$^5F_3^0$ and $^3F_2$–$^3F_2^0$ transitions, respectively. The very strong emission line around 598 nm can assign $^7F_0$–$^7D_1^0$ and/or $^3F_3$–$^5F_2^0$ transitions.

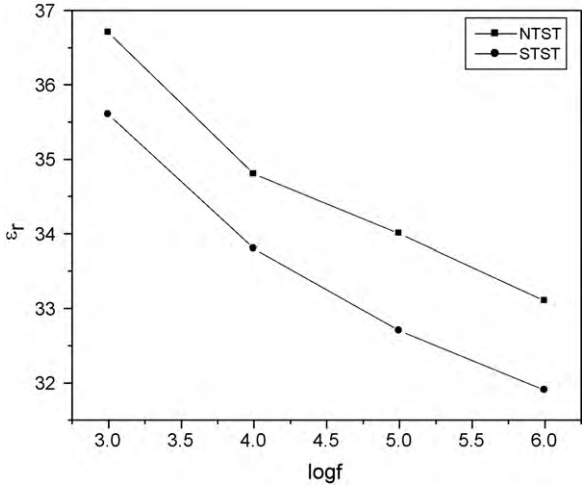

Fig. 5. Variation in ε_r with log f, in the radio frequency region.

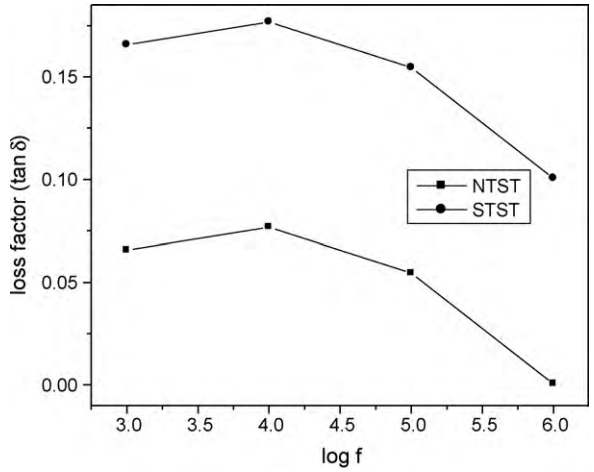

Fig. 7. Variation in loss factor (tan δ) with respect to log f.

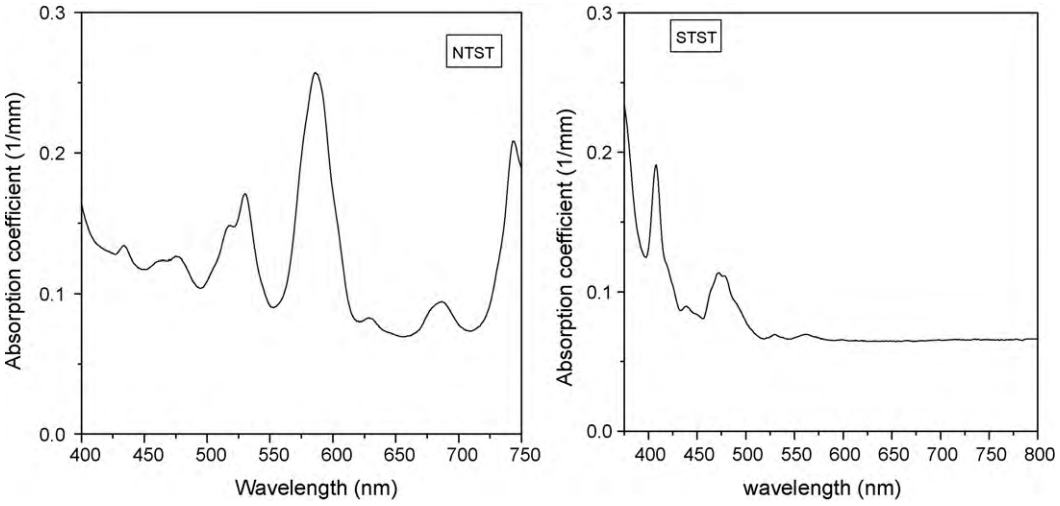

Fig. 8. Absorption spectra of NTST and STST.

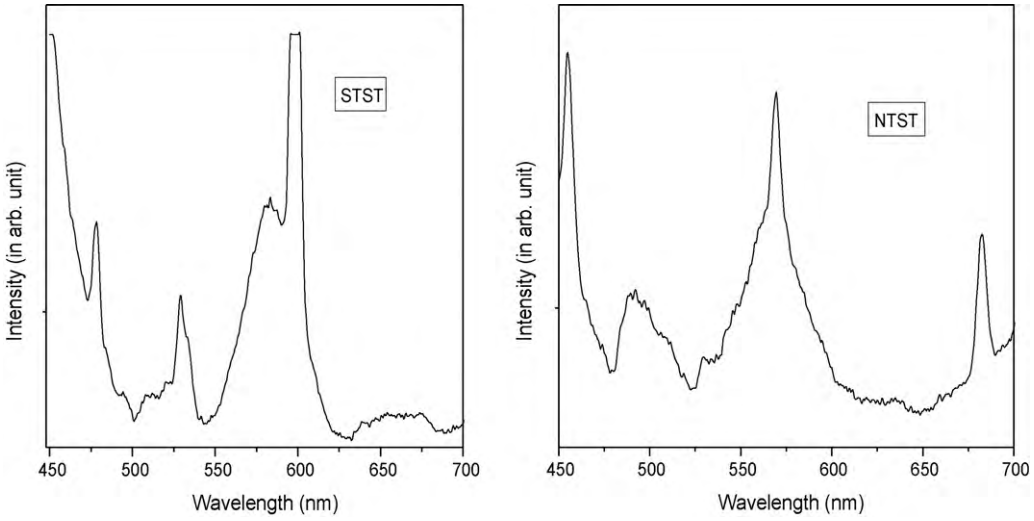

Fig. 9. Photoluminescence spectra of NTST and STST.

4. Conclusions

The $Nd(Ti_{0.8}Sn_{0.2})TaO_6$ (NTST) and $Sm(Ti_{0.8}Sn_{0.2})TaO_6$ (STST) ceramics are prepared through the conventional solid-state ceramic route. The compounds are characterized using X-ray diffraction analysis, Raman spectral analysis, scanning electron microscopy and EDS analysis. The prominent phase in both the samples is the aeschynite orthorhombic structure. Small proportion of euxenite structure is also exhibited by both the compounds. The proportion of euxenite structure is more in STST than in NTST. The dielectric properties in the radio as well as in the microwave frequencies are studied. The photoluminescence property of the samples is also analyzed. A correlation study is done between the structure and measured properties. The materials can be suitable for the fabrication of devices in microwave and optical communication.

Acknowledgements

I acknowledge University Grants Commission for Postdoctoral research award. I am grateful to Dr. M.T. Sebastian, Dr. Annamma John, Dr. J.K. Thomas and my students for their help.

References

[1] V.V. Kazantsev, E.I. Krylov, A.K. Borisov, A.I. Chupin, Russian J. Inorg. Chem. 19 (1974) 506.
[2] C.E. Holcombe, J. Mater. Sci. Lett. 14 (1974) 2255.
[3] C.E. Holcombe, M.K. Morrow, D.D. Smith, D.A. Carpenter, Survey Study of Low Expanding, High Melting, Mixed Oxides, Y-1913, Union Carbide Corporation, Nuclear Division, Oak Ridge, TN, 1974.
[4] M. Maeda, T. Yamamura, T. Ikeda, Jpn. J. Appl. Phys. 26 (1987) 76.
[5] K.P. Surendran, S. Solomon, M.R. Varma, P. Mohanan, M.T. Sebastian, J. Mater. Res. 17 (2002) 2561.
[6] K.P. Surendran, M.R. Varma, P. Mohanan, M.T. Sebastian, J. Am. Ceram. Soc. 86 (10) (2003) 1695.
[7] S. Solomon, Manoj Kumar, K.P. Surendran, M.T. Sebastian, P. Mohanan, Mater. Chem. Phys. 67 (2001) 291.
[8] T. Oishi, A. Kan, H. Ohsato, H. Ogawa, J. Eur. Ceram. Soc. 26 (2006) 2075.
[9] T. Oishi, H. Ogawa, A. Kan, H. Ohsato, J. Eur. Ceram. Soc. 25 (2005) 2889.
[10] H. Padma Kumar, J.K. Thomas, M.R. Varma, S. Solomon, J. Alloys Compd. 455 (2008) 475.
[11] H. Padma Kumar, J.T. Joseph, J.K. Thomas, K. Joy, S. Solomon, J. Mater. Sci.: Mater. Electron. 20 (2009) 551.
[12] H. Padma Kumar, C. Vijayakumar, J.K. Thomas, M.R. Varma, S. Solomon, Mater. Res. Bull. 44 (2009) 276.
[13] J.T. Joseph, H. Padma Kumar, M.R. Varma, J.K. Thomas, S. Solomon, Mater. Lett. 62 (2008) 1064.
[14] H.P. Kumar, Shyla Joseph, J.K. Thomas, M.R. Varma, S. Solomon, Int. J. Appl. Ceram. Technol. 5 (2008) 347.
[15] S. Solomon, H.P. Kumar, L. Jacob, J.K. Thomas, M.R. Varma, J. Alloys Compd. 461 (2008) 675.

[16] H.P. Kumar, J.T. Joseph, J.K. Thomas, M.R. Varma, A. John, S. Solomon, Mater. Sci. Eng. B 143 (2007) 51.
[17] H. Padma Kumar, M.K. Suresh, J.K. Thomas, B. George, S. Solomon, J. Alloys Compd. 478 (2009) 648.
[18] K. Wakino, K. Minai, H. Tamura, J. Am. Ceram. Soc. 67 (1984) 278.
[19] X. Qi, H.G. Gallagher, T.P.J. Han, B. Henderson, J. Cryst. Growth 180 (1997) 73.
[20] L. Jacob, H. Padma Kumar, K.G. Gopchandran, J.K. Thomas, S. Solomon, J. Mater. Sci.: Mater. Electron. 18 (2007) 831.
[21] H. Padma Kumar, S. George, J.K. Thomas, S. Solomon, J. Mater. Sci.: Mater. Electron. 21 (2010) 27.
[22] G.J. Thorogood, M. Avdeev, B.J. Kennedy, J. Solid State Sci., doi:10.1016/j.solidstatesciences.2010.02.036.
[23] S. Solomon, D.B. Dhwajam, G.R. Remya, A. John, J.K. Thomas, J. Alloys Compd., doi:10.1016/j.jallcom.2010.05.075.
[24] D.B. Dhwajam, J.K. Thomas, K. Joy, S. Solomon, J. Mater Sci.: Mater. Electron., doi:10.1007/s10854-010-0147-2.
[25] C.W.A. Paschoal, R.L. Moreira, C. Fantini, M.A. Pimenta, K.P. Surendran, M.T. Sebastian, J. Euro. Ceram. Soc. 23 (2003) 2661.
[26] R. Payling, P. Larkins, Optical Emission Lines of the Elements, John Wiley, New York, 2000.